

medium 1640 (RPMI) and the co-culture was done in RPMI with 10% fetal bovine serum (FBS). Where indicated, EBV-B cells were fixed in 1% formaldehyde in PBS for 10 min on ice, then washed in PBS. Peptides were synthesized either on the Pioneer Peptide Synthesizer (PE Biosystem) or on the AMS 222 multiple peptide synthesizer (Gilson) using standard fluoren-9-yl-methoxycarbonyl chemistry. The molecular masses of peptides were verified on a mass spectrometer (Bio-Synthesis Inc.).

Site-directed mutagenesis

Point mutations were introduced with a Quick Change Site-Directed Mutagenesis kit from Stratagene in accordance with the manufacturer's protocol.

HPLC fractionation of synthetic and acid-stripped peptides

COS-A3 and COS-A3/FGF-5 were prepared by retrovirally transducing COS-7 cells. Each cell line was cultured in T175 flasks and the peptides were stripped by adding to each flask 7.5 ml of citrate buffer (0.13 M citric acid, 0.056 M sodium phosphate dibasic pH 3.1) for 90 s. Peptide solutions (from about 4×10^9 cells, about 1,200 ml each) were prepared and were concentrated on a Sep-pak Plus C18 column (Waters). After freeze-drying and resolubilization into 200 μ l of a mixture of 5% acetonitrile and 0.05% (v/v) trifluoroacetic acid, peptides were fractionated on a C18 HPLC column (218TP54; Grace Vydak) using a linear gradient from 5% acetonitrile with 0.05% (v/v) TFA to 40% acetonitrile with 0.05% (v/v) TFA (1% min⁻¹ and 1 ml min⁻¹). Fractions (1 ml each) were collected, freeze-dried, reconstituted in 100 μ l RPMI and added to EBV-B cells. After incubation for 3 h, CTLs in 100 μ l RPMI with 20% FBS were added and IFN- γ was measured at 20 h. Synthetic peptides (20 μ g 9-mer and 100 μ g 49-mer) were fractionated by HPLC and assayed in the same way as above. All the 9-mer fractions were diluted 1:100 before the assay.

Antigen-processing pathway analysis

The RCC cell line was prepared by retroviral transduction with genes for HLA-A2, CIITA and a melanoma antigen gp100.

Treatment with clasto-lactacystin β -lactone (Calbiochem): RCC cells were treated with citric acid buffer (pH 3.1) for 90 s and washed, then cultured in 10 μ M clasto-lactacystin β -lactone for 3 h. After washing, T cells were added and IFN- γ was measured at 20 h.

TAP-1 dependence analysis: the same RCC line as above was infected with either an adenovirus encoding green fluorescent protein or the TAP-1 inhibitor ICP47 (multiplicity of infection = 100; 2 h). After washing, overnight culture and treatment of the RCC cells with the citric acid buffer as above, T cells were added. IFN- γ was measured at 20 h.

Received 11 September; accepted 10 November 2003; doi:10.1038/nature02240.

1. Yewdell, J. W., Reits, E. & Neefjes, J. Quantitating the MHC class I antigen processing pathway. *Nature Rev. Immunol.* **3**, 952–961 (2003).
2. Hanada, K., Perry-Lalley, D. M., Ohnmacht, G. A., Bettinotti, M. P. & Yang, J. C. Identification of fibroblast growth factor-5 as an overexpressed antigen in multiple human adenocarcinomas. *Cancer Res.* **61**, 5511–5516 (2001).
3. Carrington, D. M., Auffret, A. & Hanke, D. E. Polypeptide ligation occurs during post-translational modification of concanavalin A. *Nature* **313**, 64–67 (1985).
4. Paulus, H. Protein splicing and related forms of protein autoprocesing. *Annu. Rev. Biochem.* **69**, 447–496 (2000).
5. Rammensee, H., Bachmann, J., Emmerich, N. P., Bachor, O. A. & Stevanovic, S. SYFPEITHI: database for MHC ligands and peptide motifs. *Immunogenetics* **50**, 213–219 (1999).
6. Huang, W. M. *et al.* A persistent untranslated sequence within bacteriophage T4 DNA topoisomerase gene 60. *Science* **239**, 1005–1012 (1988).
7. Buset, M., Seledtsov, I. A. & Solov'yev, V. V. Analysis of canonical and non-canonical splice sites in mammalian genomes. *Nucleic Acids Res.* **28**, 4364–4375 (2000).
8. Steimle, V., Otten, L. A., Zufferey, M. & Mach, B. Complementation cloning of an MHC class II transactivator mutated in hereditary MHC class II deficiency (or bare lymphocyte syndrome). *Cell* **75**, 135–146 (1993).
9. Evans, T. C. Jr, Benner, J. & Xu, M. Q. The *in vitro* ligation of bacterially expressed proteins using an intein from *Methanobacterium thermoautotrophicum*. *J. Biol. Chem.* **274**, 3923–3926 (1999).
10. Min, W. & Jones, D. H. *In vitro* splicing of concanavalin A is catalyzed by asparaginyl endopeptidase. *Nature Struct. Biol.* **1**, 502–504 (1994).
11. McCracken, A. A. & Brodsky, J. L. Evolving questions and paradigm shifts in endoplasmic-reticulum-associated degradation (ERAD). *BioEssays* **25**, 868–877 (2003).
12. Bacik, I. *et al.* Introduction of a glycosylation site into a secreted protein provides evidence for an alternative antigen processing pathway: transport of precursors of major histocompatibility complex class I-restricted peptides from the endoplasmic reticulum to the cytosol. *J. Exp. Med.* **186**, 479–487 (1997).
13. Mosse, C. A. *et al.* The class I antigen-processing pathway for the membrane protein tyrosinase involves translation in the endoplasmic reticulum and processing in the cytosol. *J. Exp. Med.* **187**, 37–48 (1998).

Supplementary Information accompanies the paper on www.nature.com/nature.

Acknowledgements We thank J. R. Bennink and P. F. Robbins for suggestions, comments and encouragement; J. P. Riley and M. R. Parkhurst for the peptide synthesis, and S. A. Rosenberg for continuous support.

Competing interests statement The authors declare that they have no competing financial interests.

Correspondence and requests for materials should be addressed to K.H. (khanada@nih.gov) or J.C.Y. (jamesyang@mail.nih.gov).

Ras regulates assembly of mitogenic signalling complexes through the effector protein IMP

Sharon A. Matheny¹, Chiyuan Chen¹, Robert L. Kortum², Gina L. Razidlo², Robert E. Lewis² & Michael A. White¹

¹Department of Cell Biology, UT Southwestern Medical Center, 5323 Harry Hines Boulevard, Dallas, Texas 75390-9039, USA

²Eppley Institute for Research in Cancer and Allied Diseases, Department of Pathology, University of Nebraska Medical Center, Omaha, Nebraska 68198-6805, USA

The signal transduction cascade comprising Raf, mitogen-activated protein (MAP) kinase kinase (MEK) and MAP kinase is a Ras effector pathway that mediates diverse cellular responses to environmental cues and contributes to Ras-dependent oncogenic transformation. Here we report that the Ras effector protein Impedes Mitogenic signal Propagation (IMP) modulates sensitivity of the MAP kinase cascade to stimulus-dependent activation by limiting functional assembly of the core enzymatic components through the inactivation of KSR, a scaffold/adaptor protein that couples activated Raf to its substrate MEK¹. IMP is a Ras-responsive E3 ubiquitin ligase that, on activation of Ras, is modified by auto-polyubiquitination, which releases the inhibition of Raf–MEK complex formation. Thus, Ras activates the MAP kinase cascade through simultaneous dual effector interactions: induction of Raf kinase activity and derepression of Raf–MEK complex formation. IMP depletion results in increased stimulus-dependent MEK activation without alterations in the timing or duration of the response. These observations suggest that IMP functions as a threshold modulator, controlling sensitivity of the cascade to stimulus and providing a mechanism to allow adaptive behaviour of the cascade in chronic or complex signalling environments.

IMP was identified as a Ras-interacting protein from a *Xenopus* yeast two-hybrid screen using the Ras effector loop variant G12V/E37G (compromised for Raf interaction) as bait (GenBank accession number AY331413). The association was specific, as IMP did not interact with other effector loop variants, nor with any other Ras family G protein tested (Fig. 1a and data not shown). Truncation analysis identified a domain of 104 amino acids as minimally sufficient to mediate the two-hybrid interaction with Ras. Using

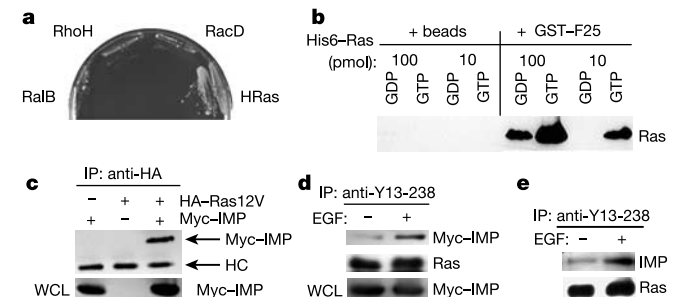


Figure 1 IMP is a Ras effector. **a**, IMP selectively associates with H-Ras in yeast. **b**, Recombinant His₆-Ras-GTP binds directly to GST-F25 (corresponding to residues 273–377 of IMP) *in vitro*. **c**, Co-immunoprecipitation of Myc-IMP with HA-Ras12V from NIH3T3 cells stably expressing HA-RasG12V. **d**, Stimulus-dependent co-immunoprecipitation of Myc-IMP with endogenous Ras from HeLa cells. **e**, Stimulus-dependent co-immunoprecipitation of endogenous IMP with endogenous Ras from HeLa cells.

recombinant proteins, we found that this domain binds directly to human H-Ras in a GTP-dependent manner (Fig. 1b). The full-length human orthologue (GenBank accession number AY332222), isolated from a Jurkat T-cell library, associated with oncogenic Ras and mitogen-activated Ras in cells (Fig. 1b–d). Notably, wild-type IMP formed a stimulus-induced complex with wild-type Ras in human cells (Fig. 1e), suggesting it is a Ras effector protein.

The primary structure of IMP suggests that it has a RING-H2 domain, followed by a ubiquitin-protease-like zinc-finger (UBP-ZnF) and leucine heptad repeats that are predicted to form a coiled-coil (SMART, Simple Modular Architecture Research Tool, <http://smart.embl-heidelberg.de>). This architecture is similar to the RING-B box coiled-coil (RBCC) family of proteins that includes the proto-oncogenes TIF-1 and PML². IMP was previously reported as a BRCA1-interacting protein 2 (Brp2) that binds the polybasic nuclear localization signal of BRCA1; however, the relevance of the interaction is unknown³. IMP is highly conserved across eukaryotes, with a single orthologue present in each species (Supplementary Fig. S1a). Multiple human tissue northern blot analysis

showed broad tissue expression (data not shown), as previously described in mouse³ and human.

Given that several Ras effector pathways collaborate with the Raf/MAP kinase cascade to induce oncogenic transformation⁴, we examined the potential contribution of IMP to Ras signalling. We expressed IMP together with the oncogenic Raf variant RafBxB⁵, or the constitutively active MEK variant MEKR4F, and examined the effect on downstream signal output. IMP inhibited focus formation of RafBxB-transformed NIH3T3 cells (data not shown), blocked Raf-induced activation of endogenous MEK and extracellular signal regulated kinase (ERK), and blocked Raf-induced accumulation of c-Fos; however, IMP did not inhibit MEKR4F signalling (Fig. 2a). The inhibitory effect of IMP seemed to be selective for Raf, as the activity of another MAP3K family protein kinase, MEKK3, was not affected by IMP expression (Fig. 2a). IMP blocked Raf signalling but did not seem to block activation of Raf, as neither a Ras-dependent activating and phosphorylation event on serine 338 (ref. 6 and Fig. 2b), nor Raf kinase activity (Fig. 2a, c), was inhibited by IMP. On the contrary, phosphorylation of S338 was enhanced. As IMP

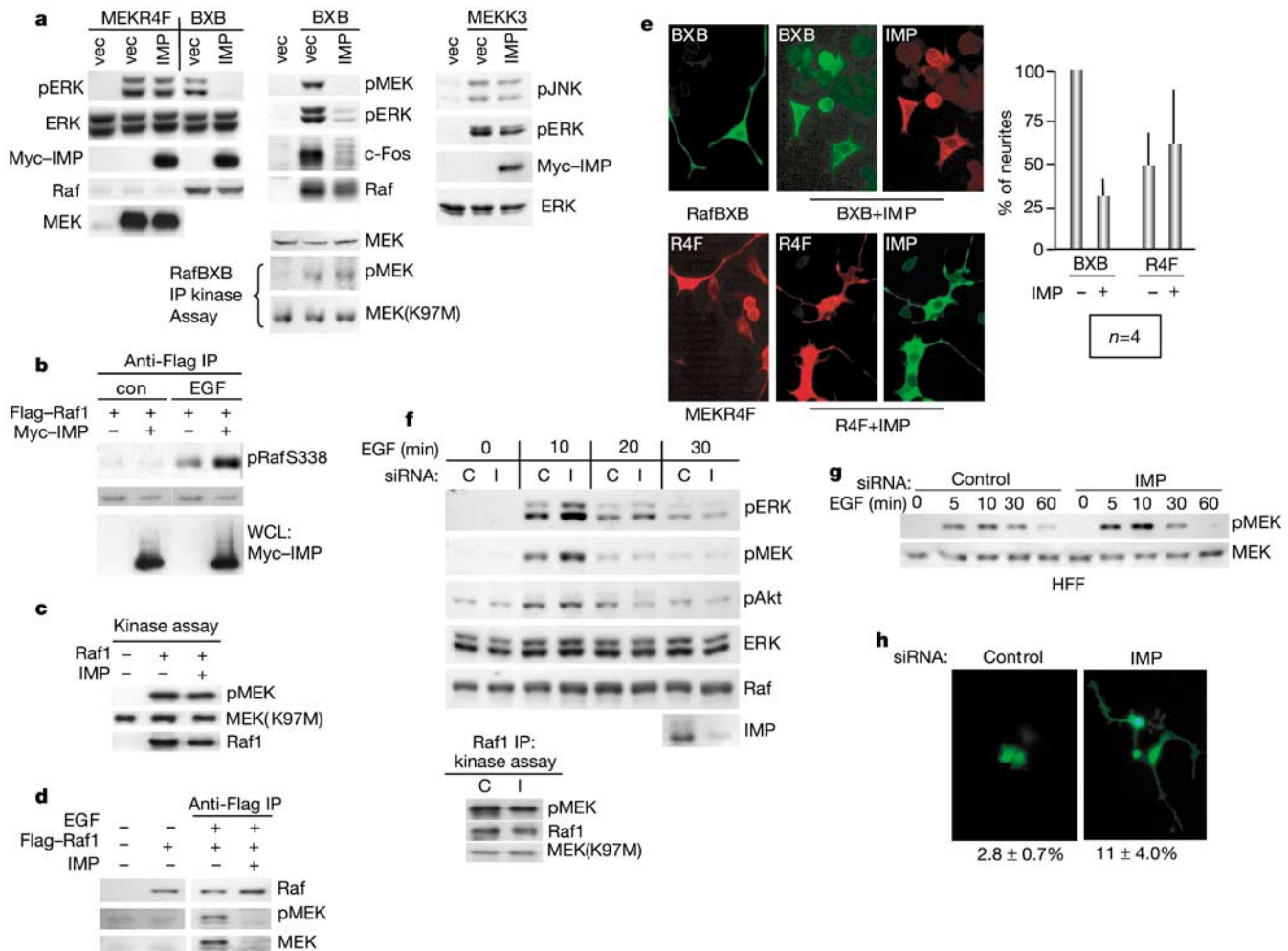


Figure 2 IMP impedes signal transmission from Raf to MEK. **a**, The effect of IMP expression on activation of MEK and ERK by RafBxB, activation of ERK by MEKR4F, and activation of ERK and JNK by MEKK3 was assessed by activation-specific (phosphorylation-specific) antibodies (pERK, pMEK and pJNK). The kinase activity of immunoprecipitated RafBxB was evaluated *in vitro* by using recombinant MEK(K97M) as a substrate. **b, c**, The effect of IMP expression on stimulus-dependent Raf1 phosphorylation and activation was evaluated with an antibody specific for Raf1 phosphorylation on S338 (**b**) and by *in vitro* kinase reactions (**c**), as described in **a**. WCL, whole-cell lysates. **d**, IMP blocks stimulus-dependent Raf–MEK association. **e**, IMP inhibits RafBxB- but not

MEKR4F-induced PC12 neurite-like extensions. Shown is the normalized percentage of cells that had extensions greater than two cell bodies in length. **f**, Depletion of IMP in HeLa cells. Cells were transfected with control (C) siRNA or siRNA targeting human IMP (I) and stimulated with EGF. Endogenous Raf1 kinase activity was assayed *in vitro* as described in **a, g**. Depletion of IMP in primary HFFs, treated as described in **f, h**. Depletion of IMP in PC12 cells. Cells were transfected with siRNAs plus GFP and treated with 10 ng ml⁻¹ NGF. GFP-positive cells were scored for the presence of neurite-like extensions as described in **e**.

blocks ERK activation, this last observation was probably a consequence of uncoupling negative feedback inhibition of epidermal growth factor (EGF) signalling. However, IMP did block mitogen-induced association of Raf1 with endogenous MEK1 and MEK2

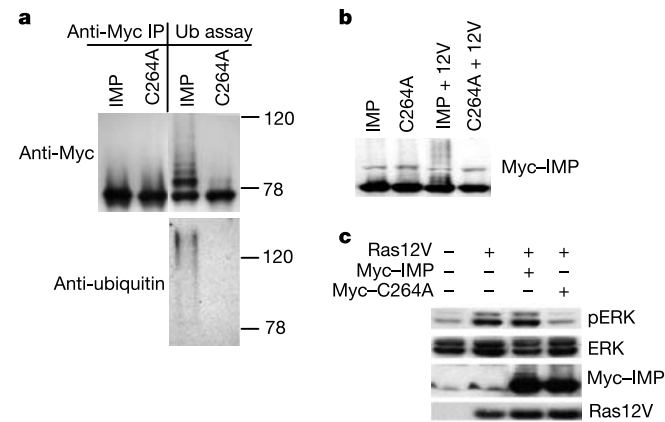


Figure 3 IMP is a Ras-sensitive RING-H2 E3 ubiquitin ligase. **a**, Immunoprecipitated Myc-IMP or Myc-IMP(C264A) was mixed with minimal essential purified ubiquitin ligase components, minus an E3 ligase, *in vitro*. IMP auto-ubiquitination was detected by immunoblotting. **b**, Ras12V enhances auto-ubiquitination of IMP. Whole-cell lysates were immunoblotted as shown. **c**, Ligase-defective IMP(C264A), but not wild-type IMP, can block ERK activation by oncogenic Ras.

(MEK1/2; Fig. 2d). Thus, IMP inhibits signal propagation through Raf by uncoupling activated Raf from its downstream substrates MEK1/2. This inhibition translates to downstream cellular responses, as shown by the capacity of IMP to block Raf-induced immediate early gene expression (Fig. 2a) and Raf-induced neurite-like differentiation of PC12 cells (Fig. 2e).

To validate the hypothesis that IMP is a negative regulator of Raf kinase signalling, we depleted IMP in various cell types. In human epithelial cells and primary human fibroblasts, depletion of IMP did not increase baseline ERK activity in serum-starved cells, but did increase the amplitude of the response of the MAP kinase cascade to mitogen stimulation (Fig. 2f, g). The duration of MEK activation was not appreciably altered, suggesting that IMP does not contribute to immediate early negative feedback control but, instead, limits the absolute capacity of the system to respond to ligand stimulation. EGF signalling was not generally increased on inhibition of IMP expression, as activation of AKT was unaffected (Fig. 2f). The capacity of IMP to modulate ERK activation negatively was also conserved in *Drosophila* S2 cells (Supplementary Fig. S2). These observations suggest that IMP adds impedance or resistance to signal propagation through Raf to MEK, thereby modulating the cellular threshold of sensitivity to stimulus. Consistent with this, we found that short interfering RNAs (siRNAs) targeting rat IMP enhanced the sensitivity of PC12 cells to suboptimal doses of nerve growth factor (NGF), as evaluated by morphological differentiation (Fig. 2h).

A potential functional motif in IMP is the putative RING-H2

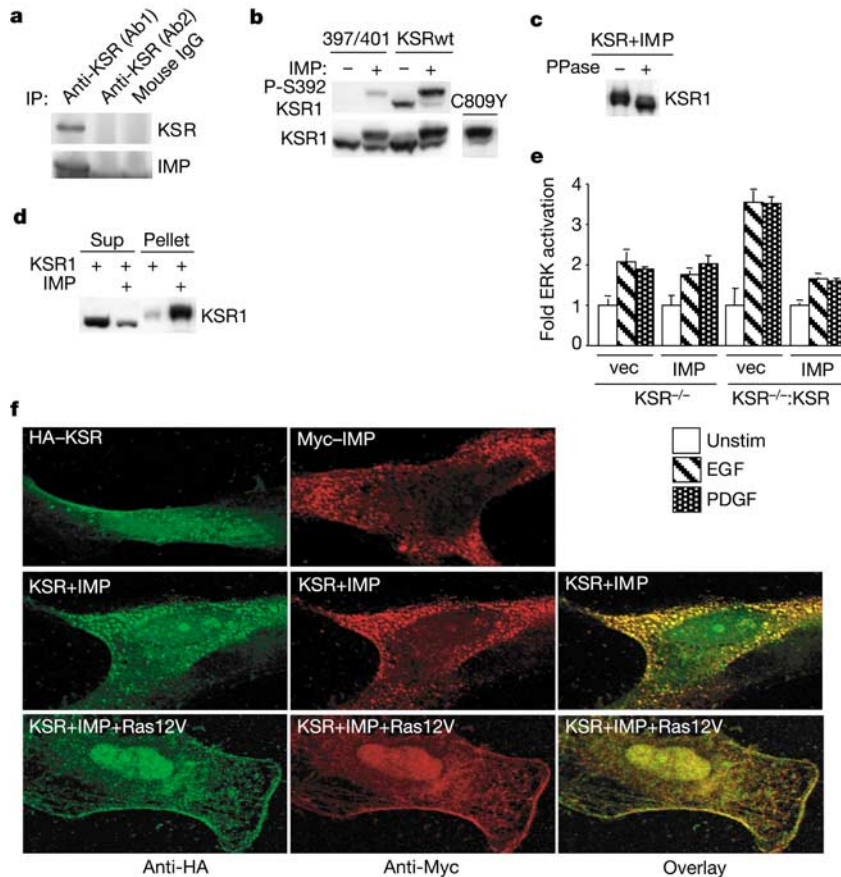


Figure 4 IMP inactivates KSR. **a**, Endogenous IMP co-immunoprecipitates with endogenous KSR from rat brain lysates. An ineffective KSR antibody (Ab2) and 'normal' IgG were used as controls. **b**, Effect of IMP expression on the mobility and inhibitory phosphorylation of KSR1. Whole-cell lysates were immunoblotted to detect KSR and the indicated KSR variants. Phosphorylation of S392 was detected with a phosphorylation-specific antibody. **c**, IMP induces hyperphosphorylation on KSR1. HA-KSR1 was

immunoprecipitated from the insoluble fraction (see **d**) and treated with phosphatase. **d**, High-molecular-mass KSR is insoluble in Triton. HEK293 cell lysates were separated into Triton-soluble and Triton-insoluble fractions. Equal amounts of protein were loaded. **e**, IMP inhibition of ERK activation is dependent on KSR. **f**, IMP and KSR1 colocalize in Ras-sensitive Triton-insoluble structures.

domain (Supplementary Fig. S1c). In many proteins, this domain facilitates protein ubiquitination through E3 ubiquitin ligase activity⁷. To examine whether IMP has E3 ubiquitin ligase activity, immunoprecipitated IMP or an IMP variant, in which the first cysteine in the RING-H2 consensus sequence was changed to alanine (C264A), was assayed for ligase activity by a standard *in vitro* reconstitution assay. IMP became polyubiquitinated *in vitro* in a RING-domain-dependent manner in the presence of recombinant E1, UbcH4 (E2) and ubiquitin (Fig. 3a). Thus, IMP is associated with E3 ubiquitin ligase activity and, like most E3 ligases, seems to be an auto-substrate *in vitro*.

We did not detect IMP-dependent modification of H-Ras, Raf1, MEK1 or ERK1 (data not shown). However, IMP is probably a *bona fide* target for its own E3 ligase activity in cells, as indicated by the appearance of a 'ladder' of high-molecular-mass IMP species in mitogen-stimulated cells and in cells expressing Ras12V together with IMP (Fig. 3b). This was not observed with the ligase-defective C264A mutant (Fig. 3b) and suggests that IMP E3 ligase activity is regulated by Ras. In contrast to RafBXB, IMP did not inhibit oncogenic Ras activation of MAP kinase. However, inactivation of the E3 ligase domain of IMP exposed inhibitory activity (Fig. 3c). These observations show that IMP inhibition of the Raf kinase cascade is Ras sensitive. Therefore, Ras is probably coupled to the MAP kinase cascade through dual effector interactions that mediate activation of Raf kinase together with derepression of Raf-MEK complex formation.

We considered that IMP might interfere with formation of the Raf-MEK complex through steric inhibition resulting from the competitive association of IMP with Raf and/or MEK, similar to the mechanism of action suggested for Raf kinase inhibitory protein (RKIP)⁸. However, we did not detect any substantial interaction of IMP with Raf1 or MEK1, either by yeast two-hybrid or by immunoprecipitation of ectopically expressed proteins (data not shown). KSR1 is an adaptor/scaffold protein that functions, at least in part, to couple Raf to MEK^{1,9,10}. As IMP uncouples Raf from MEK, we examined whether IMP affects the MAP kinase cascade at the level of KSR. In cells, IMP associated with KSR through the respective amino-terminal halves of the two proteins (Supplementary Fig. S3) and an endogenous KSR-IMP complex was detected (Fig. 4a). Although the dynamics of KSR function in cells is not well understood, studies suggest that KSR responds to signalling events. For example, KSR in cells is phosphorylated on several sites, some of which are modified in a mitogen-dependent manner^{9,11}. The serine/threonine protein kinase c-Tak-1 phosphorylates KSR on S392, and this modification can inactivate the scaffolding function of KSR in cells⁹. Furthermore, a KSR variant (C809Y), identified as the product of a loss-of-function KSR mutant in *Caenorhabditis elegans*¹², is hyperphosphorylated, fails to associate with MEK, and partitions to a Triton-insoluble fraction¹³.

We found that expression of IMP together with KSR resulted in a marked accumulation of a higher-molecular-mass species of KSR, mimicking the effects of the inactivating C809Y mutation (Fig. 4b). The IMP-induced modification of KSR was hyperphosphorylation, as indicated by phosphatase treatment (Fig. 4c), and, like KSR(C809Y), the hyperphosphorylated form partitioned to a Triton-insoluble cell fraction (Fig. 4d). Although phosphorylation of KSR on S392 was slightly enhanced by IMP, a KSR variant defective for c-Tak-1 association (I397A/V401A)⁹ showed that c-Tak-1-independent phosphorylation events on KSR accumulate in the presence of IMP (Fig. 4b). KSR^{-/-} fibroblasts isolated from knockout mice show reduced activation of ERK in response to various stimuli, as compared with wild-type cells¹, which can be enhanced by low ectopic expression of KSR (R.L.K and R.E.L., unpublished results). We used this system to examine whether IMP requires KSR to inhibit ERK activation. IMP did not inhibit EGF- or platelet-derived growth factor (PDGF)-stimulated ERK activation in KSR-null cells; however, IMP eliminated the capacity of KSR to

enhance ERK activation (Fig. 4e). Although the mechanistic consequences of the IMP-induced modifications of KSR are unknown, they are consistent with the behaviour of inactive KSR and suggest that IMP maintains KSR in an inactivated state. Immunostaining showed colocalization of IMP and KSR in Triton-resistant punctate structures (Fig. 4f), suggesting that IMP may recruit KSR to microdomains inaccessible to activators of KSR function. Expression of oncogenic Ras reversed this phenotype, further supporting the hypothesis that Ras inactivates IMP (Fig. 4f).

In summary, we have identified IMP, a Ras effector that negatively regulates MAP kinase activation by limiting the formation of Raf-MEK complexes. The mechanism of inhibition seems to be inactivation of the KSR1 adaptor/scaffold protein, showing that, in addition to promoting signal transmission, scaffold proteins can function to restrict signal propagation. Ras can inactivate IMP through induction of IMP auto-ubiquitination, facilitating KSR-dependent engagement of MEK by activated RAF. These observations show that Ras has dual effector inputs to the MAP kinase cascade: induction of Raf kinase activity, which is concomitant with derepression of KSR-dependent Raf-MEK complex formation. This relationship provides a mechanism to limit engagement of the MAP kinase cascade in the absence of Ras activation. MAP kinase activation contributes to many diverse cellular responses to the environment. The capacity to control the amplitude of this response through molecules such as IMP probably contributes to flexible and adaptive cellular behaviour in the context of complex regulatory signals. □

Methods

Expression vectors and antibodies

Expression vectors are given in the Supplementary Information. All primary antibodies were obtained from Santa Cruz Biotech except for those against HA.11 (Babco), Ras (Transduction Laboratories), Raf phosphorylated on S338 (Upstate Biotech), JNK1/2 phosphorylated on T183/Y185 (Cell Signalling), c-Fos (Upstate Biotech) and KSR (Transduction Laboratories). Antibodies against MEK1/2, MEK1/2 phosphorylated on S218/S222, ERK1/2 and ERK1/2 phosphorylated on T202/Y204 were from Sigma. All Raf immunodetection was done with a C-12 anti-Raf antibody (Santa Cruz Biotech) except for that in Fig. 2e, which used an anti-Raf1 monoclonal antibody (Pharmingen). Anti-IMP was generated against the carboxy-terminal peptide KLPSRKGRSKRGK (Biocarta). Antibody against KSR1 phosphorylated on S392 was generated against a peptide corresponding to S392 of KSR1 and its flanking residues (LRRTES(PO₃)/VPSD). We used the following secondary antibodies: horseradish peroxidase (HRP)-conjugated goat anti-mouse, HRP-conjugated goat anti-rabbit, fluorescein isothiocyanate (FITC)-conjugated goat anti-mouse and rhodamine-conjugated goat-rabbit (all from Jackson Laboratories). Anti-HA, anti-Y13-238 and anti-Myc9E10 agarose conjugates were from Santa Cruz Biotech. Anti-Flag M2 agarose was from Sigma.

Cell culture and transfection

Cell culture conditions are given in the Supplementary Information. Plasmid DNA was transfected by using calcium phosphate precipitation for NIH3T3 and HEK293 cells, and by using Lipofectamine 2000 (Promega) for HeLa and PC12 cells. siRNAs were transfected by using Oligofectamine (Promega). We treated S2 cells with double-stranded RNA as described¹⁴.

In vitro binding and ubiquitin ligase assays

The *in vitro* binding assay is described in the Supplementary Information. For the ubiquitin ligase assay, immunoprecipitated Myc-IMP or Myc-IMP(C264A) was added to purified assay components, comprising 5 μ M bovine ubiquitin (Sigma), 0.33 μ M E1, 13 nM recombinant human UbcH4, energy regeneration mix and ligase buffer (50 mM Tris (pH 7.5), 150 mM KCl and 1 mM MgCl₂), and mixed for 1.5 h at 37 °C.

RNA interference

HeLa cells and human foreskin fibroblasts (HFFs) were transfected with 100 pmol of annealed siRNA oligonucleotides targeting human IMP, or mouse Caveolin1 as a control, essentially as described¹⁵. To obtain high (>90%) transfection efficiencies with the primary fibroblasts, cells were briefly exposed to trypsin (Gibco), before transfection using Oligofectamine (Promega) as described¹⁶. After 24 h, the cells were stimulated with 1 ng ml⁻¹ EGF (Sigma) and then lysed by boiling in SDS-Tris for immunoblotting. Similar results were obtained with siRNAs targeting two non-overlapping sites on IMP. PC12 cells were transfected with 100 pmol of annealed siRNAs targeting mouse Caveolin1 or rat IMP, together with an expression plasmid encoding green fluorescent protein (GFP). After 48 h, cells were treated with 10 ng ml⁻¹ NGF (Sigma) and incubated for an additional 24 h. We scored GFP-positive cells for the presence of neurite-like extensions (Supplementary Information).

Immunoprecipitation

See Supplementary Information for the detailed protocol. In brief, cells were lysed in Nonidet P-40 (NP-40) buffer and cleared by centrifugation at 4 °C. Antibody-conjugated agarose was added to the supernatant and incubated at 4 °C for 3 h or overnight. Beads were washed four times in NP-40 buffer plus 500 mM NaCl. Co-immunoprecipitations were treated in the same way, except that the beads were washed in NP-40 buffer without salt.

Immunofluorescence

Cells were washed with PBS and fixed in 3.7% formaldehyde. Permeabilization, washes and antibody dilutions were done with 1% calf serum and 0.25% Triton X-100 in PBS. Primary antibodies were diluted 1:80. FITC-conjugated goat anti-mouse was used at a dilution of 1:300, and goat anti-rabbit was used at 1:1,000. For the experiments in Fig. 4f, the cells were washed with PBS then incubated in cold 0.1% Triton in PBS for 10 min at 4 °C. The cells were then fixed and immunostained as described above. All images were captured at a magnification of $\times 40$ on a confocal microscope (Leica).

For fluorescence *in situ* ERK activation assays (Fig. 4e), cells were stained with antibodies against phosphorylated ERK1/2 (Cell Signalling, diluted 1:100) and antibodies against ERK1 (Santa Cruz, 1:100), followed by AlexaFluor-680-conjugated anti-mouse (Molecular Probes, 1:100) and IRDye800-conjugated anti-rabbit (Rockland, 1:100) secondary antibodies. Signal detection and quantification were done by the Odyssey system (Li-Cor) as directed by the manufacturer.

In situ ERK activation assay

We infected KSR1^{-/-} cells with bicistronic retroviruses encoding KSR1-IRES-GFP and IMP-IRES-YFP or control viruses, and sorted them for green and yellow fluorescence by FACS. Sorted cells were seeded at 1.5×10^4 cells per well in 96-well plates 24 h before analysis. Cells at 70% confluence were deprived of serum for 4 h, and treated with 100 ng ml⁻¹ EGF or 25 ng ml⁻¹ PDGF for 5 min, before being assayed for ERK activation by a quantitative fluorescence *in situ* plate assay.

Phosphatase and Raf kinase assays

See Supplementary Information for the phosphatase assays. For the Raf kinase assays, Raf1 or RafBxB was immunoprecipitated and washed five times in NP-40 buffer, once in PBS, and once in 25 mM HEPES (pH 7.5) and 10 mM MgCl₂. The beads were then added to kinase assay reagents comprising 10 mM MgCl₂, 83 μ M ATP, 25 mM HEPES (pH 7.5) and 50 ng μ l⁻¹ recombinant MEK (K94A). The reaction was incubated at 30 °C for 40 min with regular mixing, and stopped on the addition of 2 \times sample buffer.

Received 1 October; accepted 14 November 2003; doi:10.1038/nature02237.

1. Nguyen, A. *et al.* Kinase suppressor of Ras (KSR) is a scaffold which facilitates mitogen-activated protein kinase activation *in vivo*. *Mol. Cell Biol.* **22**, 3035–3045 (2002).
2. Jensen, K., Shiels, C. & Freemont, P. S. PML protein isoforms and the RBCC/TRIM motif. *Oncogene* **20**, 7223–7233 (2001).
3. Li, S. *et al.* Identification of a novel cytoplasmic protein that specifically binds to nuclear localization signal motifs. *J. Biol. Chem.* **273**, 6183–6189 (1998).
4. White, M. A. *et al.* Multiple Ras functions can contribute to mammalian cell transformation. *Cell* **80**, 533–541 (1995).
5. Bruder, J. T., Heidecker, G. & Rapp, U. R. Serum-, TPA-, and Ras-induced expression from Ap-1/Ets-driven promoters requires Raf-1 kinase. *Genes Dev.* **6**, 545–556 (1992).
6. Diaz, B. *et al.* Phosphorylation of Raf-1 serine 338/serine 339 is an essential regulatory event for Ras-dependent activation and biological signalling. *Mol. Cell Biol.* **17**, 4509–4516 (1997).
7. Joazeiro, C. A. & Weissman, A. M. RING finger proteins: mediators of ubiquitin ligase activity. *Cell* **102**, 549–552 (2000).
8. Yeung, K. *et al.* Suppression of Raf-1 kinase activity and MAP kinase signalling by RKIP. *Nature* **401**, 173–177 (1999).
9. Muller, J. S. O., Copeland, T., Pivnicka-Worms, H. & Morrison, D. K. C-TAK1 regulates Ras signalling by phosphorylating the MAPK scaffold, KSR1. *Mol. Cell* **8**, 983–993 (2001).
10. Roy, F., Laberge, G., Douziche, M., Ferland-McCollough, D. & Therrien, M. KSR is a scaffold required for activation of the ERK/MAPK module. *Genes Dev.* **16**, 427–438 (2002).
11. Brennan, J. A., Volle, D. J., Chaika, O. V. & Lewis, R. E. Phosphorylation regulates the nucleocytoplasmic distribution of kinase suppressor of Ras. *J. Biol. Chem.* **277**, 5369–5377 (2002).
12. Sundaram, M. & Han, M. The *C. elegans* KSR-1 gene encodes a novel Raf-related kinase involved in Ras-mediated signal transduction. *Cell* **83**, 889–901 (1995).
13. Stewart, S. *et al.* Kinase suppressor of Ras forms a multiprotein signalling complex and modulates MEK localization. *Mol. Cell Biol.* **19**, 5523–5534 (1999).
14. Clemens, J. C. *et al.* Use of double-stranded RNA interference in *Drosophila* cell lines to dissect signal transduction pathways. *Proc. Natl Acad. Sci. USA* **97**, 6499–6503 (2000).
15. Elbashir, S. M. *et al.* Duplexes of 21-nucleotide RNAs mediate RNA interference in cultured mammalian cells. *Nature* **411**, 494–498 (2001).
16. Chien, Y. & White, M. A. RAL GTPases are linchpin modulators of human tumour-cell proliferation and survival. *EMBO Rep.* **4**, 800–806 (2003).

Supplementary Information accompanies the paper on www.nature.com/nature.

Acknowledgements This work was supported by grants from the National Cancer Institute (to M.A.W. and to R.E.L.) and the Welch Foundation, and by an Idea Development award (to M.A.W.).

Competing interests statement The authors declare that they have no competing financial interests.

Correspondence and requests for materials should be addressed to M.A.W. (michael.white@utsouthwestern.edu).

Mustard oils and cannabinoids excite sensory nerve fibres through the TRP channel ANKTM1

Sven-Eric Jordt¹, Diana M. Bautista¹, Huai-hu Chuang¹, David D. McKemy¹, Peter M. Zygmunt³, Edward D. Högestätt³, Ian D. Meng^{2*} & David Julius¹

¹Department of Cellular and Molecular Pharmacology and ²Department of Neurology, University of California, San Francisco, California 94143-2140, USA
³Department of Clinical Pharmacology, Institute of Laboratory Medicine, Lund University Hospital, SE-221 85 Lund, Sweden

* Present address: Department of Physiology, College of Osteopathic Medicine, University of New England, 11 Hills Beach Road, Biddeford, Maine 04005, USA

Wasabi, horseradish and mustard owe their pungency to isothiocyanate compounds. Topical application of mustard oil (allyl isothiocyanate) to the skin activates underlying sensory nerve endings, thereby producing pain, inflammation and robust hypersensitivity to thermal and mechanical stimuli^{1,2}. Despite their widespread use in both the kitchen and the laboratory, the molecular mechanism through which isothiocyanates mediate their effects remains unknown. Here we show that mustard oil depolarizes a subpopulation of primary sensory neurons that are also activated by capsaicin, the pungent ingredient in chilli peppers, and by Δ^9 -tetrahydrocannabinol (THC), the psychoactive component of marijuana. Both allyl isothiocyanate and THC mediate their excitatory effects by activating ANKTM1, a member of the transient receptor potential (TRP) ion channel family recently implicated in the detection of noxious cold^{3,4}. These findings identify a cellular and molecular target for the pungent action of mustard oils and support an emerging role for TRP channels as ionotropic cannabinoid receptors^{5–8}.

Capsaicin and mustard oil are plant-derived natural products that elicit pain and inflammation when applied to the skin^{1,2}. These effects are produced by the depolarization of sensory nerve fibres that detect noxious stimuli (so-called nociceptors). In addition to transmitting ‘pain signals’ to the spinal cord, nociceptors may also release peptides—such as substance P and calcitonin-gene-related peptide (CGRP)—peripherally to produce vascular leakage and vasodilation, leading to inflammation and tenderness at the site of irritant application^{9,10}. Capsaicin mediates these effects by activating the vanilloid receptor TRPV1, a heat-sensitive cation channel on nociceptor terminals^{11–13}. TRPV1 belongs to the greater family of TRP channels, many of which are key components of signal transduction pathways in a variety of sensory systems^{14–16}.

Topical administration of mustard oil also produces nociceptor excitation, but whether this occurs through a direct action on sensory neurons or through a specific membrane receptor is not known¹⁷. TRPV1-deficient mice retain sensitivity to mustard oil, indicating that capsaicin and isothiocyanates excite nociceptors through distinct molecular mechanisms¹⁸. However, inflammatory responses to these irritants show partial cross-desensitization, suggesting that they act through convergent cellular signalling pathways^{19,20}.

To identify the cellular site of action of mustard oil, we used calcium imaging to ask whether allyl isothiocyanate (20 μ M) excites dissociated sensory neurons from rat trigeminal ganglia. Approximately 35% of cultured neurons showed rapid and robust increases in intracellular free calcium with the application of this compound (Fig. 1). Subsequent exposure to capsaicin (1 μ M) excited a larger cohort of neurons (~55%), encompassing all of the mustard-oil-responsive cells. Capsaicin-evoked responses result from an influx of divalent cations directly through the TRPV1 channel²¹. Similarly,